

Feedforward Construction of the Receptive Field and Orientation Selectivity of Visual Neurons in the Pigeon

Da-Peng Li, Qian Xiao and Shu-Rong Wang

Laboratory for Visual Information Processing, State Key Laboratory of Brain and Cognitive Sciences, Institute of Biophysics, Chinese Academy of Sciences, Beijing 100101, People's Republic of China

How the receptive field (RF) of visual cells is formed and how to explain the orientation selectivity have been intensely studied and debated. Here we provided direct electrophysiological evidence by single-unit recording and electrophysiological mapping that the elongated excitatory RF of a visual cell in the pigeon nucleus isthmi is constructed from aligned circular excitatory RFs of tectal cells, whereas its inhibitory RF originates from intranuclear inhibitory circuits. The orientation selectivity of an isthmic cell is mainly determined by its excitatory RF and sharply tuned by its inhibitory RF. Retrograde tracing showed that the tectal cells converging onto an isthmic cell are arranged in a narrow dorsoventral column in the tectum. According to the retinotopic map on the tectum, the excitatory RFs of these tectal cells are aligned in a line orthogonal to the horizontal meridian of the visual field in agreement with the result obtained by electrophysiological mapping.

Keywords: feedforward convergence, nucleus isthmi, optic tectum, orientation selectivity, visual system

Introduction

Hubel and Wiesel (1962) proposed that the elongated receptive field (RF) of a simple cortical cell is constructed from aligned concentric RFs of afferents from the lateral geniculate nucleus (LGN), and this elongated RF underlies the orientation selectivity of cortical cells. This feedforward model has been supported by several subsequent studies. The finding that the RFs of LGN afferents are aligned with the preferred orientation of the cortical region they target was demonstrated by Chapman and others (1991) at the level of a cortical column and by Reid and Alonso (1995) at the level of a single cell. Ferster and others (1996) showed that the convergence of thalamic inputs was enough to explain the orientation selectivity of cortical cells. However, these studies were unable to provide direct electrophysiological and anatomical evidence whether these LGN cells would converge onto a single cortical cell probably because of anatomical and physiological complexities of the geniculocortical system in mammals.

The tecto-isthmic system in birds may be a good model for directly showing feedforward convergence of RFs and neuronal mechanisms underlying the orientation selectivity of visual cells for 2 reasons. First, the tectofugal and the thalamofugal pathways in birds are 2 parallel pathways from the retina to the telencephalon, which are homologous to the colliculo-pulvinar-cortical and geniculocortical pathways in mammals, respectively (Karten 1969; Shimizu and Bowers 1999). However, the most important for visual tasks is the tectofugal pathway in nonmammals such as pigeons, whereas it is the thalamofugal pathway in mammals. In addition, the optic tectum in the tectofugal pathway has reciprocal connections with the mid-

brain nucleus isthmus (NI), which is homologous to the parabrachial nucleus that is reciprocally connected with the superior colliculus in mammals. The avian NI is divided into 2 independent subnuclei, the nucleus isthmi pars magnocellularis (Imc) and the nucleus isthmi pars parvocellularis (Ipc), both of which are visual centers (see Wang 2003). Surprisingly, the RF organization in the tecto-isthmic system is quite similar to that in the geniculocortical system (Fig. 1). Like LGN cells, tectal cells possess a round or oval RF consisting of concentric excitatory (ERF) and inhibitory (IRF) receptive fields (Jassik-Gerschenfeld and Guichard 1972; Frost and others 1981; Gu and others 2000); isthmic cells are similar to cortical cells in having an elongated RF (Wang and Frost 1991; Wang and others 1995). These suggest that the elongated RF of an isthmic cell may be constructed from aligned tectal RFs, and this elongated RF may underlie the orientation selectivity of isthmic cells. Second, there is plenty of knowledge available about retinal representation on the tectum and topographical projections between the tectum and NI, both of which are easily accessible for electrodes (McGill and others 1966; Bilge 1971; Hunt and Künzle 1976; Güntürkün and Remy 1990; Wang and Frost 1991; Gu and others 2000; Wang and others 2000, 2004, 2006). In addition, we are able to precisely map RF on the screen and manipulate tectal and isthmic cells (Wang and others 2000; Yang and others 2002; Wu and others 2005).

Therefore, the present study was undertaken by using single-unit recording, computer mapping, and anatomical tracing techniques in order to provide direct physiological and anatomical evidence for the feedforward model of RFs and explore the neuronal mechanisms underlying the orientation selectivity of visual cells.

Materials and Methods

Forty-two pigeons (*Columba livia*) were used in physiological and anatomical studies following the guidelines regarding the care and use of animals established by the Society for Neuroscience. In physiological studies, each of 29 pigeons was anesthetized with urethane (20%, 1 ml/100 g body weight) and then placed in a stereotaxic apparatus. The left tectum was surgically exposed, and the overlying dura mater was excised. The right eye was kept open and the left covered. A screen of 130 degrees vertical \times 140 degrees horizontal was placed tangential to and 40 cm away from the viewing eye. A pigeon normally holds its head with the bill angled down 34 degrees relative to the horizontal meridian of the visual field (Erichsen and others 1989), whereas this angle is 72 degrees when the pigeon is stereotaxically fixed, the horizontal meridian was thus rotated counterclockwise from the pigeon's view by 38 degrees (Britto and others 1990; Fu and others 1998) to meet the normal angle between the horizontal meridian and the pigeon's bill (Fig. 2).

Three types of visual stimuli were generated by a computer with graphics-card (Ti 4600, MicroStar) and back-projected with a projector (PG-M20X, Sharp) on the screen: 1) A black square of 1-4 degrees was

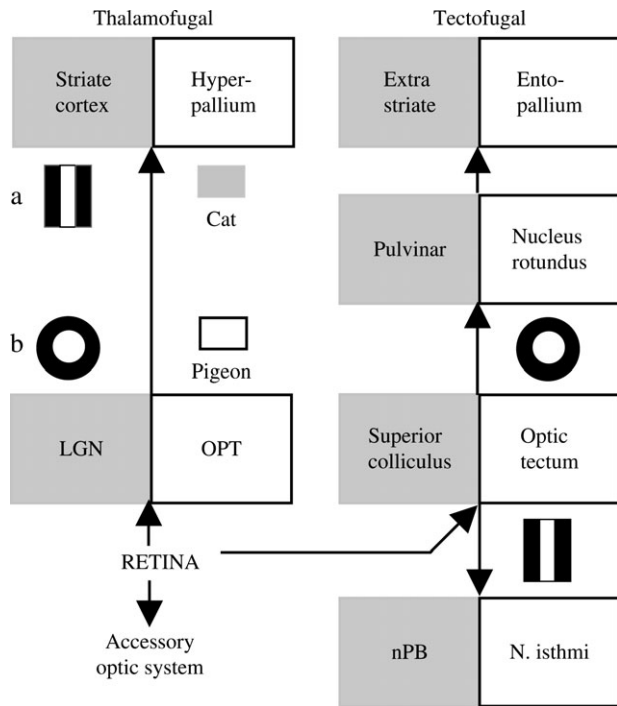


Figure 1. Schematic diagram shows the similarities of feedforward visual pathways in birds and mammals. The thalamofugal and tectofugal pathways are 2 parallel pathways from the retina to the telencephalon in the pigeon, which are homologous to the geniculocortical and colliculo-pulvinar-cortical pathways in the cat, respectively. The accessory optic system in both species is also similar but not detailed for brevity. Side by side IRF (black) and ERF (white) (a) exist in cortical and isthmic cells, whereas concentric IRF and ERF (b) exist in visual cells in LGN and tectum. nPB, the parabigeminal nucleus; and others see text. The pathways are drawn based on Karten (1969), Shimizu and Bowers (1999), and Reiner and others (2004).

moved at 20–40 degrees/s randomly along a series of parallel paths covering the whole screen to map the ERF and IRF of tectal or isthmic cells (Wang and others 2000; Yang and others 2002; Wu and others 2005). They were color coded (Fig. 2) and thus were encompassed by an equal-color line (i.e., equal-rate line) with the Magic Wand Tool of the software Adobe Photoshop (Version 7.0, Adobe Systems Inc, San Jose, CA). Because the variability in the spontaneous rate of 10 isthmic neurons in 5 pigeons recorded over 20 s was $14 \pm 2\%$, we used a criterion of 20% change in firing rate to represent an index of change. Thus, the equal-rate line of 20% higher and lower than the spontaneous rate encompassed an ERF and IRF, respectively. The areal size of ERF and IRF was measured with the measure function of the software Image-Pro Plus (Version 4.5.0.19, Media Cybernetics Inc, Silver Spring, MD). It can automatically measure the size of an area selected. This stimulus was also used to measure the directional selectivity of Imc cells by moving at 20–40 degrees/s in 8 directions spaced by 45 degrees with nasal-0 degree. 2) Double squares (1–4 degrees each) were used to plot the IRF in nonspontaneous cells, one of which was moved in the ERF, whereas the other moved outside with increasing distance between (Frost and others 1981; Wang and others 2000). The inhibitory strength of IRF was described by the inhibitory ratio $= (f_1 - f_2)/f_1$, where f_1 and f_2 were the firing rate evoked by motion of a single stimulus in ERF and that by simultaneous motion in both ERF and IRF. 3) To measure the orientation selectivity of isthmic cells, a bar (2×30 degrees) was moved at 30 degrees/s in the sensitive directions with its orientation relative to long axis (0 degree) of ERF changing in steps of 22.5 degrees (Fig. 5). The sharpness of an orientation-tuning curve was described by its half-width at half-height. In all experiments, the luminance of black and white was 0.1 and 6.6 cd/m^2 , respectively.

A single-barreled pipette ($\sim 2 \mu\text{m}$ tip diameter) filled with 2 M sodium acetate and 2% pontamine skyblue (Hellon 1971; Gu and others 2001) was used for recording neuronal activity and marking electrode tip sites.

A 2-barreled pipette was also used, the recording barrel of which was filled as above and the other was filled with lidocaine hydrochloride (2%) or bicuculline methiodide (Sigma Chemical Co, St. Louis, MO, 20 mM, pH = 3.5) and connected to a pneumatic picopump (PV800, Medical Systems Corp, Greenvale, NY) or a microiontophoresis unit for drug application (Wang and others 2000). Spatial overlap of a tectal RF with an isthmic RF was a precondition for examining effect of tectal blockade on the isthmic cell. Therefore, an isthmic RF was mapped with single-barreled pipette, and then a tectal cell was recorded with the recording barrel of 2-barreled pipette whose RF overlapped the isthmic RF. To examine whether tectal RFs would converge onto an isthmic RF, lidocaine as a sodium-channel blocker was sequentially pressure injected (50–100 nl) to block activity of several tectal cells with RFs overlapping the isthmic RF one after another. If tecto-isthmic feedforward convergence exists, the isthmic RF would be locally deleted in those areas that corresponded topographically to RFs of tectal cells whose activity was blocked. To explore where an isthmic IRF may originate from, the RF of an isthmic cell was mapped with 2-barreled pipette, and then bicuculline as an antagonist to γ aminobutyric acid A (GABA_A) receptors was iontophoretically applied by current (50–100 nA) to remove GABAergic inputs to this isthmic cell. Changes in the IRF extents and inhibitory strength of this cell were determined. Tectal and isthmic cells were isolated according to the pigeon's brain atlas (Karten and Hodos 1967). Neuronal spikes were analyzed by averaging firing rates accumulated in 4–6 repeats with the computer. Because firing rates evoked by identical stimuli were different from cell to cell, they were normalized by the firing ratio $= f_1/f_2$, where f_2 and f_1 were the maximal firing rate and a submaximal rate. These ratios were used to plot statistical diagrams for a group of cells. In some experiments, the recording sites were marked with dye iontophoretically deposited by negative current pulses of 10–20 μA in intensity and 0.5 s in duration at 1 Hz for 10–15 min (Gu and others 2001; Cao and others 2004).

In anatomical studies, each of 13 pigeons was anesthetized with ketamine hydrochloride (5%, 0.25 ml/100 g) and then placed in a stereotaxic apparatus. The left tectum was exposed, and the overlying dura mater was excised. A 2-barreled pipette, one barrel of which was filled with 2 M sodium acetate for recording visual activity and the other was filled with fluorescent Fluoro-Ruby (4% in saline, Molecular Probes, Eugene) for retrograde tracing, was stereotaxically advanced into Imc to find a visual cell where Fluoro-Ruby was iontophoretically applied with positive current pulses (5 μA in intensity, 0.5 s in duration, 1 Hz, 10 min) (Varoquaux and Poulain 1994; Qu and others 1996; Vercelli and others 2000). After 3–5 days' survival, the pigeon was anesthetized with urethane (20%, 2 ml/100 g) and transcardially perfused with a saline followed by 4% paraformaldehyde. The brain was removed from the skull, fixed in 4% paraformaldehyde for 6–12 h, and soaked in 30% sucrose solution in a refrigerator overnight. Coronal or oblique sections perpendicular to the horizontal axis adopted by Hamdi and Whitteridge (1954) were cut on a freezing microtome at 60 μm thickness. Alternating sections were collected for observation with a fluorescence microscope (Olympus-IX 71, 530–560 nm) or counterstained with cresyl violet for localizing the tracer injection sites and the labeled tectal cells with a microscope. The topographic distribution of labeled cells in the tectum was reconstructed with the software MicroCCD (Version 3.14, Diffraction Ltd, Ottawa, Ontario, Canada) and Adobe Photoshop (Version 7.0, Adobe Systems Inc).

Results

The RF organization of 68 isthmic and 44 tectal neurons was computer mapped and color coded with ERF in red and IRF in blue. Fifty-eight visual cells recorded in the magnocellular subnucleus of NI, Imc, were all characterized by an elongated ERF that was flanked by side by side IRF subfields. Their ERF were oriented perpendicular to the horizontal meridian of the visual field rotated by 38 degrees, with an average size of 78.2 ± 15.9 degrees in length and 12.2 ± 3.4 degrees in width, and their IRF were irregular in shape and much larger than ERF (Fig. 2). For comparison, 10 visual cells were recorded from the parvocellular subnucleus of NI, Ipc, and they all had a round

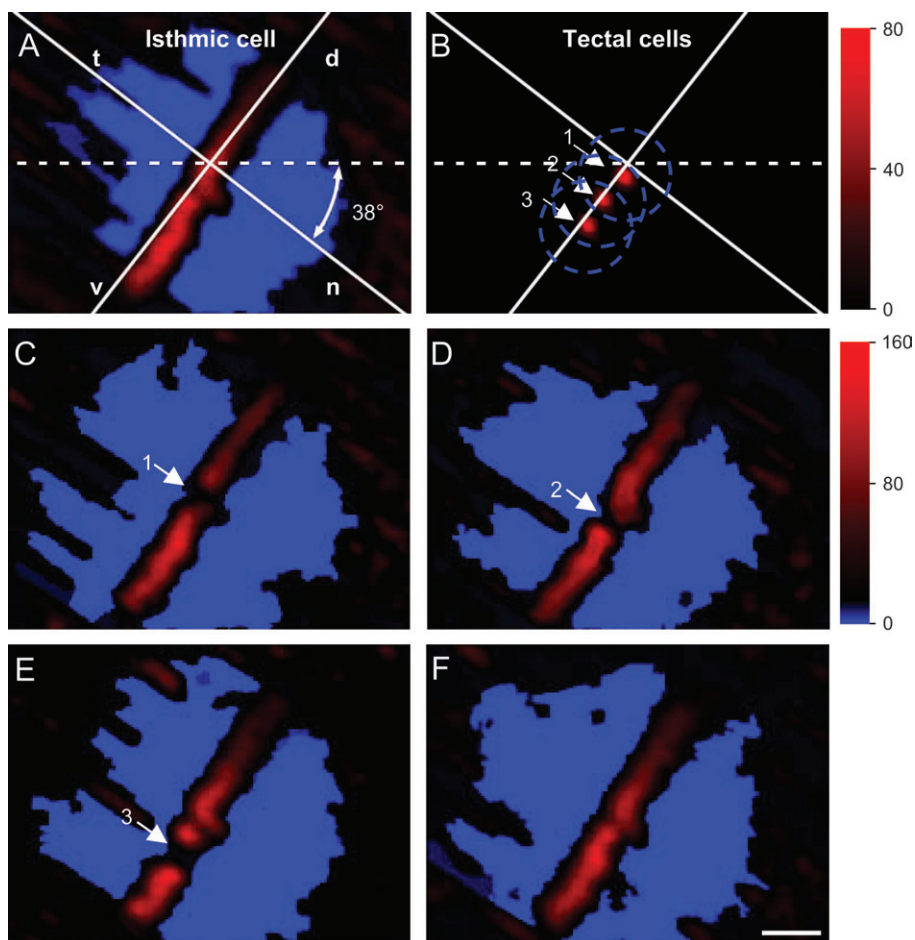


Figure 2. An elongated isthmic ERF (red) is converged from aligned circular ERF of tectal cells. It is orthogonal to the horizontal meridian of the visual field rotated by 38 degrees (n-t line) during recording and flanked by IRF subfields (A, blue). The ERF of a tectal cell overlapping the isthmic ERF was mapped, and then its recording site was blocked by lidocaine, which deleted an area in the isthmic ERF corresponding to the tectal ERF (B-1, C-1). Similarly, ERF of tectal cells 2 and 3 were sequentially mapped, and their recording sites were blocked (B-2, 3), resulting in separate deletions in the isthmic ERF (D-2, E-3). The deletions recovered 10 min after blockade (F). Dashed circles symbolize tectal IRF that could not be mapped due to low spontaneity. Letters n, t, d, and v represent nasal, temporal, dorsal, and ventral, respectively. Scales: 0–160 spikes/s in (A, C–F) and 0–80 spikes/s in (B), bar = 20 degrees.

ERF with an average size of 10.4 ± 1.7 degrees. Similarly, 44 tectal cells examined also had a small round ERF surrounded by a large IRF that was usually determined by double stimuli (see the Methods) due to no or weak spontaneous activity in these cells. The average size of tectal ERF was 8.8 ± 1.5 degrees.

It is interesting to note that RF organization of Imc cells and tectal cells is respectively comparable with that of simple cortical cells and LGN cells in mammals, and this remarkable similarity thus encouraged us to directly examine whether aligned tectal RFs could converge onto an isthmic RF with reversible blockade. The RF of an Imc cell was mapped with the computer, and then a tectal cell was isolated whose ERF overlapped the isthmic ERF. Blockade of tectal activity by lidocaine resulted in complete deletion of an area in the isthmic ERF that corresponded topographically to and was much larger than the tectal ERF in the visual field. However, the isthmic IRF was not affected by tectal blockade. In additional experiments, we recorded 10 tectal cells whose ERF were located within areas where the IRF of 5 isthmic cells were mapped. Lidocaine blockade (100 nl) of these tectal cells did not change the isthmic IRF in all cases. Figure 2 is an example showing that sequential blockade of activity in 3 tectal cells, whose ERF overlapped the ERF of an Imc cell, deleted 3 areas in the isthmic ERF but did not

affect the isthmic IRF. These deleted areas in the isthmic ERF were recovered 10 min after blockade. Figure 3 shows the relationship between spatial locations of ERF of 44 tectal cells in the visual field and those of 44 deleted areas in ERF of 21 isthmic cells during blockade of tectal activity, with one isthmic ERF being examined for blockade of 1–5 tectal cells. If the location of tectal ERF centers and that of the deleted area centers in the isthmic ERF were described by r and θ in polar coordinates, where r is the radial distance from the visual field center and θ is the counterclockwise angle from the horizontal meridian of the visual field, the relationship between both locations was fitted by a linear function $x = y$, showing that ERF of tectal cells blocked by lidocaine nicely corresponded to the deleted areas of the isthmic ERF induced by tectal blockade. These data strongly support our hypothesis that the ERF of an Imc cell is constructed by feedforward convergence of numerous tectal ERF.

However, the isthmic IRF was not changed in its inhibitory strength and areal size during blockade of tectal activity (Fig. 2C–E). For example, the inhibitory ratio of IRF in 5 Imc cells was 0.97 ± 0.04 as control and 0.99 ± 0.01 during tectal blockade, and these 2 values were not different (paired t -tests, $P = 0.45$). The IRF size of these cells obtained during tectal blockade was

98 ± 7% of control value, and statistical analysis did not show significant difference between the control and experimental values ($P = 0.59$). The finding that the inhibitory strength and size of an isthmus IRF were not affected by tectal blockade suggested that the isthmus IRF may stem from local circuits intrinsic to Imc.

We thus examined this suggestion by iontophoretically applying bicuculline as a GABAergic antagonist in the site where an Imc cell was isolated whose RF was computer mapped. As shown in Figure 4A-C, IRF of this Imc cell was completely abolished during bicuculline application within Imc, whereas its ERF was unchanged by this antagonist. Figure 4D shows statistical data obtained from 15 Imc cells whose inhibitory inputs were removed by bicuculline applied at currents of 50–100 nA. Their average inhibitory ratios were 0.93 before,

0.20 during, and 0.91 after bicuculline application. It appeared that the inhibitory strength of these cells was significantly reduced even at a lower dosage of bicuculline, indicating that inhibitory inputs to Imc cells predominantly, if not exclusively, originate within the nucleus.

The elongated ERF of isthmus cells predicted that these cells might be orientation selective. We examined the directional selectivity by moving a square in 8 directions spaced by 45 degrees and found that these cells were sensitive to motion in the temporonasal, dorsoventral, and ventrodorsal directions in the visual field rotated by 38 degrees during recording (Fig. 5A,B). The orientation selectivity is usually examined by moving a bar in the directions orthogonal to its own long axis. However, the orientation selectivity measured this way would confound the directional selectivity. Because the isthmus cells were

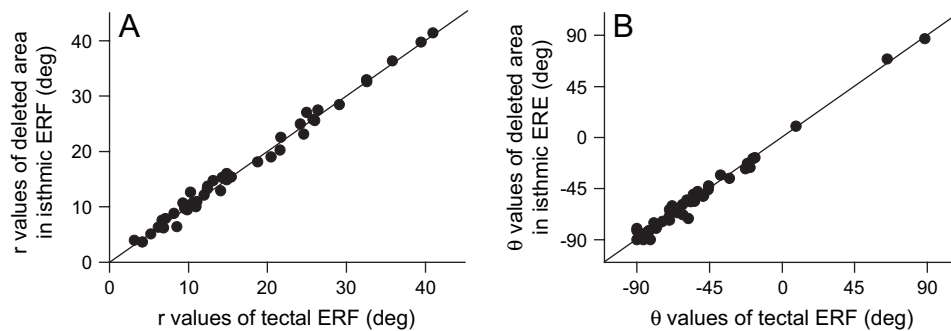


Figure 3. Relationship between the locations of 44 tectal ERF and those of 44 deleted areas in the isthmus ERF. The center locations of tectal ERF and those of deleted areas are described by r and θ in polar coordinates, where r is the radial distance from the visual field center and θ is the counterclockwise angle from the horizontal meridian of the visual field; the clockwise angle is described by negative values. Linear relationship shows that tectal ERF well correspond to the deleted areas of isthmus ERF induced by tectal blockade.

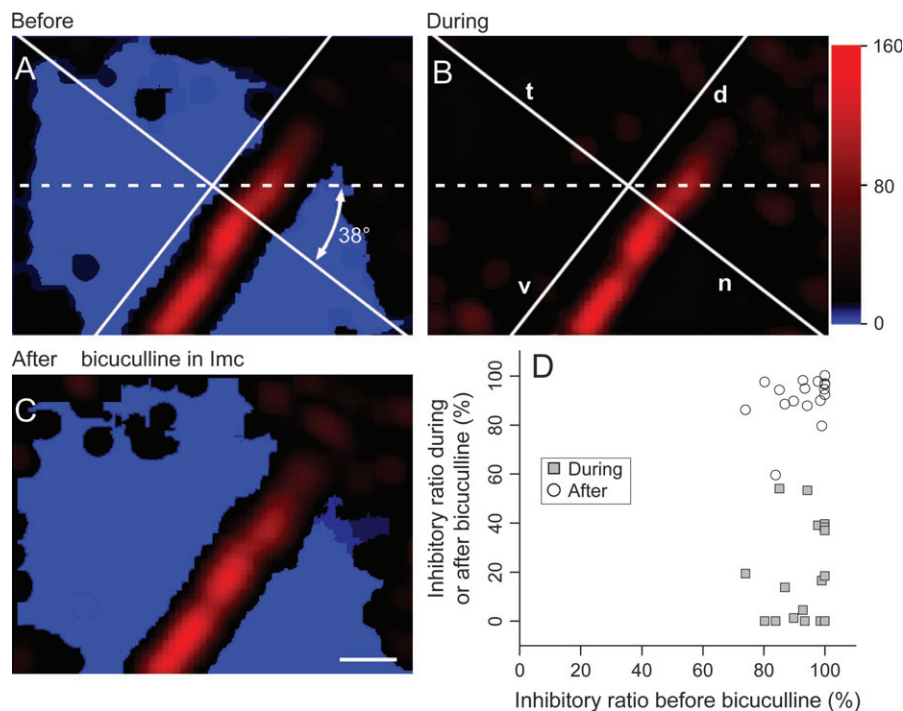


Figure 4. The IRF subfields of an isthmus cell are generated in intranuclear inhibitory circuits. The RF of an isthmus cell is composed of an ERF (red) and 2 IRF subfields (blue) (A). Inhibitory subfields were completely deleted during bicuculline application within Imc (B, 100 nA) and recovered 2 min after (C). In (D) are statistical data of 15 isthmus cells showing that their inhibitory ratio was significantly reduced during bicuculline. The horizontal meridian (dashed line) of the visual field was rotated by 38 degrees during recording (n-t line). Abbreviations see Figure 2. Scales: 0–160 spikes/s, bar = 20 degrees.

sensitive to directional motion, we thus measured the orientation selectivity by moving a bar in the sensitive directions with its orientation relative to the longitudinal axis (0 degree) of ERF changing in steps of 22.5 degrees. The orientation-tuning curves of an Imc cell were almost identical for the 3 sensitive directions (Fig. 5C). The orientation-tuning curve fitted by a Gaussian function of 10 isthmic cells was shown in Figure 5D, whose firing rates were collected for 3 sensitive directions and 9 orientations in each direction. Its half-width at half-height was 14.5 degrees, indicating that the orientation selectivity of Imc cells was sharply tuned. It appeared that this orientation

selectivity stems from the elongated ERF and side by side IRF subfields. Figure 6A shows the orientation-tuning curves of an Imc cell before, during, and after application of bicuculline within Imc, indicating that the tuning curve was considerably widened, and the maximal firing rate shifted away from 0 degree in the presence of bicuculline. Statistical data of 5 Imc cells were depicted in Figure 6B. The half-width at half-height of orientation-tuning curves before bicuculline was 16.7 degrees, whereas this half-width during bicuculline was 49.4 degrees. In other words, the half-width at half-height was increased by 196% after removal of GABAergic inputs to Imc cells. In all these

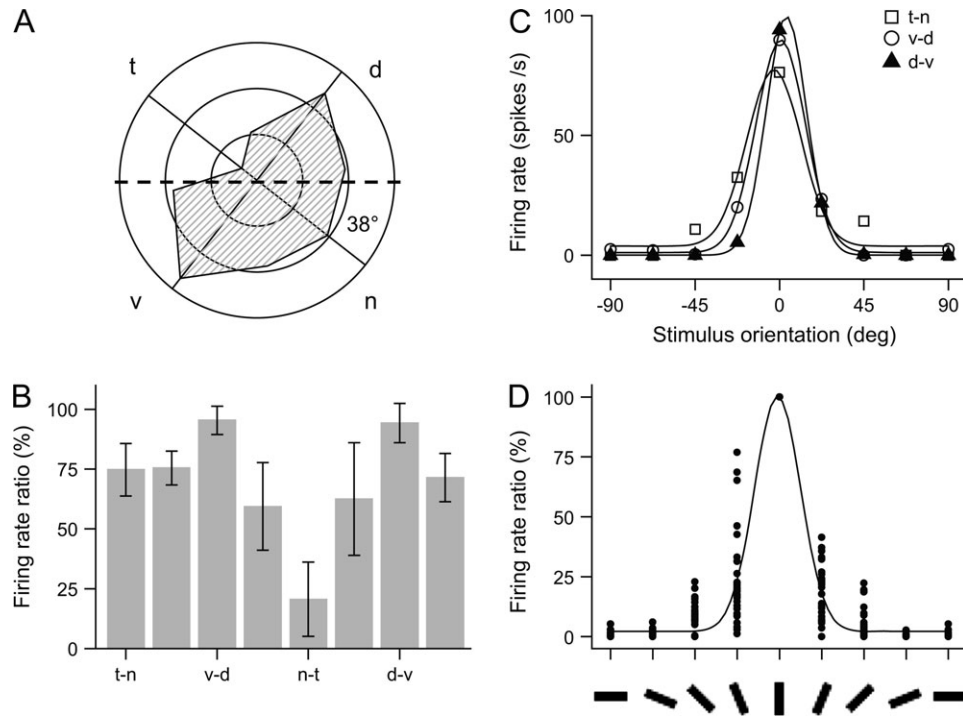


Figure 5. Isthmic cells are selective for the direction of motion and orientation of visual stimuli. Directional tuning diagram of an isthmic cell (A) and statistical histograms of 10 isthmic cells (B) show directional selectivity of isthmic cells for motion in the temporonasal (t-n), dorsoventral (d-v), and ventrodorsal (v-d) directions in the visual field whose horizontal meridian was rotated by 38 degrees during recording. The stimulus was moved at 30 degrees/s in 8 directions spaced by 45 degrees, error bars = standard deviation. In (C) are the orientation-tuning curves of an isthmic cell responding to a bar (2 × 30 degrees) moved at 30 degrees/s in 3 sensitive directions. Three repeats are averaged. In (D) is the orientation-tuning curve fitted by a Gaussian function of average firing rate ratio in 10 isthmic cells whose firing rates were collected for 3 sensitive directions and 9 orientations as shown by oriented bars. Each of the columns contains 30 data points (10 cells × 3 directions).

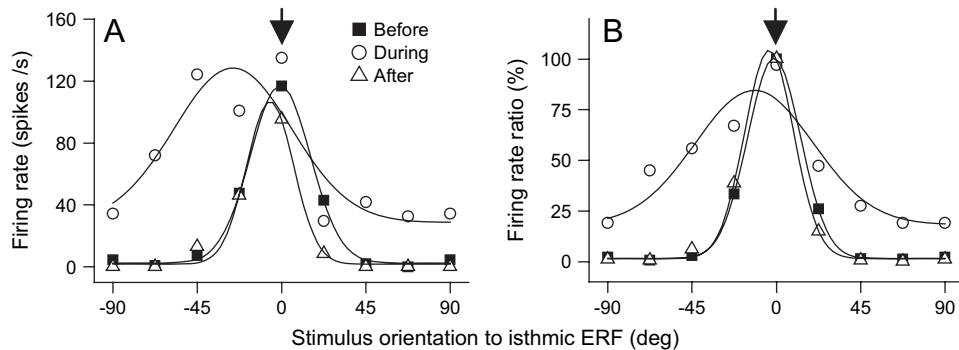


Figure 6. The orientation tuning of isthmic cells is sharpened by intranuclear inhibition. The orientation-tuning curve of an isthmic cell was considerably widened during bicuculline (100 nA) (A). Statistical data of 5 isthmic cells obtained before, during, and after bicuculline show that half-width at half-height of tuning curves was changed from 16.7 degrees as control to 49.4 degrees during bicuculline. Although the maximal responses occurred to 0 degree orientation during bicuculline (arrows), Gaussian-fitted curves peak at an orientation tilted from 0 degree due to asymmetrical responses of isthmic cells to symmetrical changes in stimulus orientation.

electrophysiological experiments, the recording sites of 22 Imc cells were marked with pontamine skyblue, and all of them were localized within the nucleus.

We then attempted to find the anatomical substrate underlying convergence of tectal RFs onto an isthmic RF by microiontophoretic administration of Fluoro-Ruby as a retrograde tracer into the site where an isthmic cell was isolated. Ninety tectal cells on average (from 52 to 130) were labeled per pigeon, and they were bipolar cells located in tectal layers 10–11, with an axon issuing from apical dendrite and then turning toward the deep tectum to give a shepherd's crook appearance (Fig. 7). To explore how these labeled cells were distributed in the tectum, the number of sections with labeled cells per pigeon and the tectal thickness occupied by one labeled cell were compared between coronal and oblique cutting methods. Coronal sections were cut in 5 pigeons, demonstrating that the labeled cells were scattered in 40 tectal sections ranging from 35 to 48 sections. On the other hand, oblique sections were cut in additional 8 pigeons, which were perpendicular to the horizontal axis adopted by Hamdi and Whitteridge (1954), showing that the labeled cells were concentrated in 9 tectal sections ranging from 6 to 13 sections. Furthermore, the tectal thickness occupied by one labeled cell was also quite different between coronal and oblique cutting

methods. This value was $30.5 \pm 8.3 \mu\text{m}$ for coronal sections, whereas it was $6.2 \pm 0.8 \mu\text{m}$ for oblique sections. Because all the injections were made with identical current parameters and the brains were cut at the same thickness, these differences in the number of sections with labeled cells and in the tectal thickness occupied by one labeled cell indicated that the tectal cells converging onto an isthmic cell were concentrated in a dorsoventral column that was perpendicular to the horizontal axis adopted by Hamdi and Whitteridge (1954) (Figs 8 and 9). Tectal cells in this column arrange their RFs perpendicular to the horizontal meridian according to the retinotopic map on the tectum (Hamdi and Whitteridge 1954), and, therefore, the RF of an isthmic cell receiving tectal afferents was elongated and perpendicular to the horizontal meridian of the visual field.

Discussion

The present study provided direct electrophysiological evidence that a group of tectal ERF is converged to construct an isthmic ERF in the pigeon as suggested by Hubel and Wiesel (1962) for the geniculocortical system in the cat. Our data showed that blockade of tectal cells with ERF overlapping an isthmic ERF deleted those areas in the isthmic ERF that corresponded topographically to the tectal ERF in the visual field. Because some tectal cells projecting to the isthmic cell were concurrently blocked in the tectal site where lidocaine was applied, the deleted area in the isthmic ERF was thus much larger than the tectal ERF in size. Though the spread of the lidocaine blockade within the tectum could not be measured because we did not have the technical tools to record multiunit activity within short distances from the center of the lidocaine injection, our results provided an indirect control indicating that the lidocaine spread was so limited that the inactivated area should be very small because only a restricted portion of the isthmic ERF was deleted with tectal blockade. Meanwhile, the isthmic IRF was not changed by tectal blockade even in cases when we injected lidocaine to inactivate the tectal cells whose ERF were located within the isthmic IRF. It is possible that inhibitory neurons within Imc are more densely interconnected than excitatory neurons and/or receive more convergent input from the tectum.

On the other hand, bicuculline applied to an isthmic cell could completely remove the isthmic IRF. It was natural to predict that the ERF extent of this cell would be more or less expanded after removal of the isthmic IRF, but it was not the case. It may imply that excitatory input from many tectal cells in a dorsoventral column to an isthmic cell is much more powerful than inhibitory input from some isthmic cells/interneurons, so that blockade of the inhibitory input could not show observable changes in the extent of the isthmic ERF (Fig. 9). Even though bicuculline may enhance the activity level of the isthmic cell which may in turn raise tectal activity, the changes in tectal activity might be unable to affect the isthmic cell in a feedback way, likely due to heterotopic projections between the Imc to tectum (Wang and others 2004). Tectal cells send excitatory but not inhibitory inputs to the isthmic cell (Wang 2003), and the isthmic cells and/or interneurons providing inhibitory inputs to the isthmic cell receive tectal inputs from a region other than the tectal site being blocked.

Therefore, the orientation selectivity of an isthmic cell may also originate both from the tectum and from Imc. The present study showed that the elongated ERF of an isthmic cell is

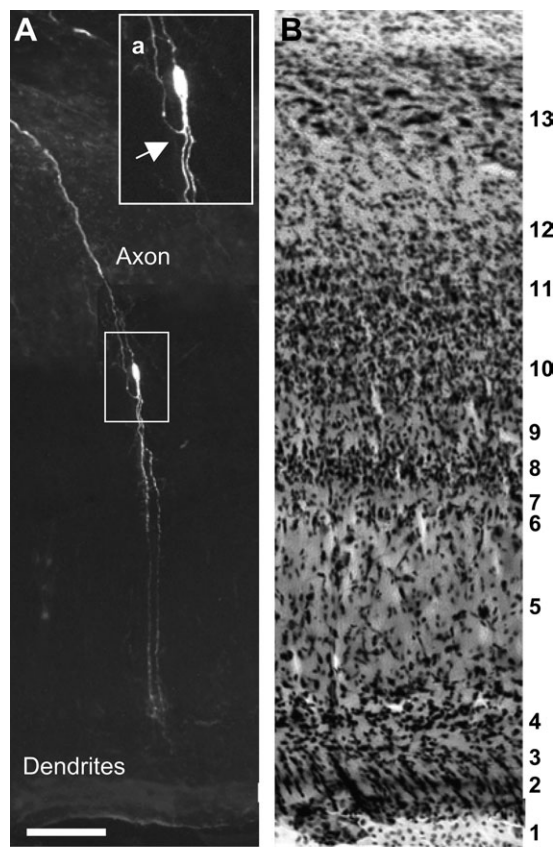


Figure 7. Morphology and location of a tectal neuron labeled by fluorescent dye applied in Imc. This radial bipolar cell in tectal layer 10 issues an axon from its apical dendrite, and the axon gives a shepherd's crook appearance (arrow). A rectangle frame in (A) is enlarged in inset (a) showing the cellular morphology in detail. Tectal lamination in (A) is determined according to neighboring Nissl-stained section (B). Numerals at the right indicate 1–13 of 15 tectal layers. Bar = 100 μm in (A) and (B), 50 μm in (a).

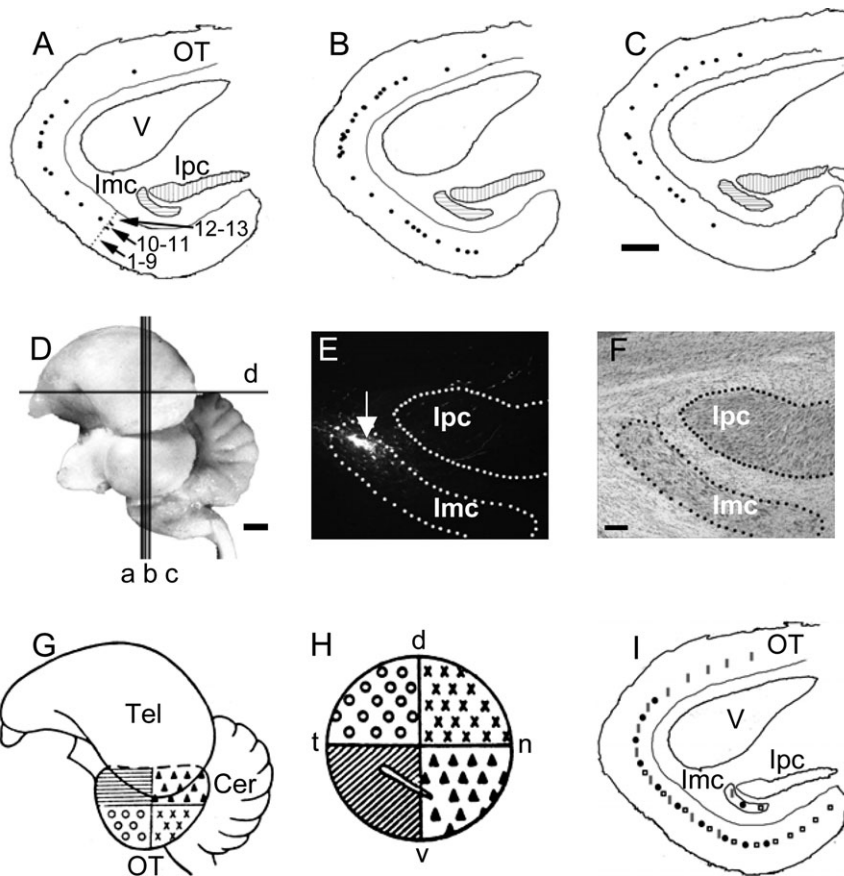


Figure 8. Topographic distribution of tectal cells labeled by dye injected in lmc. Fifty-seven cells were distributed in tectal layers 10-11 in sections (A-C) that were cut along vertical lines a-c to the horizontal line d (D). Fluorescent photograph (E) shows a dye deposit in lmc (arrow), and it is localized according to neighboring Nissl-stained section (F). Distribution of labeled tectal cells topographically corresponded to the injected sites with identical symbols (I). Retinal quadrants (H) project topographically to the optic tectum (G, OT). Cer, cerebellum; Tel, telencephalon; V, ventricle; others see text Figure 2. Numerals with arrows indicate 1-13 of 15 tectal layers. Scale bars: 1 mm in (A-C, J), 2 mm in (D), and 100 μ m in (E, F). Panels (D), (G), and (H) are based on Hamdi and Whitteridge (1954) and Karten and Hodos (1967).

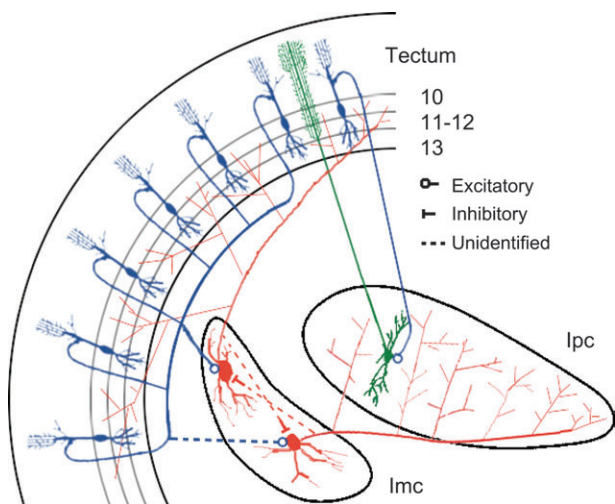


Figure 9. Schematic drawings show neural connections between neurons in the tectum (blue), lmc (red), and lpc (green). The tectum is reciprocally connected with both lmc and lpc. However, projections between the tectum and lpc are point-to-point topographically organized, whereas those between the tectum and lmc are area-to-area topographically organized. Some of lmc cells project to lpc with widely distributed axonal branches. An lmc cell may inhibit others directly or via interneurons. Numerals indicate 10-13 of 15 tectal layers. Based on Tömböl and Németh (1998), Wang and others (2004, 2006), Tömböl and others (2006), and the present results.

responsible for a major proportion of the orientation selectivity of the isthmic cell because a bar oriented parallel to the preferred orientation of the isthmic ERF evoked maximal responses in all cases. On the other hand, the isthmic IRF could sharpen the orientation tuning of the cell. After the IRF was totally removed by bicuculline, the orientation selectivity of lmc cells largely remained, but the orientation-tuning curves were considerably widened, and Gaussian-fitted curves shifted their peaks away from 0 degree because of asymmetrical responses of these cells to symmetrical orientation changes of the bar due to their asymmetrical inhibitory subfields. In normal conditions, a horizontal or oblique bar activates simultaneously ERF and IRF, and the excitation from ERF is strongly suppressed by the inhibition from large IRF. When IRF is inactivated, the isthmic cell responds to the horizontal or oblique bar although this response is weaker than the response to a vertical bar. This is exactly what we found in our results. In fact, the functional role of intracortical inhibition for the orientation selectivity of cortical cells is a matter of debate. Ferster and Miller (2000) found that the selectivity of cortical cells for stimulus orientation remained after inhibitory input was blocked, indicating that excitatory inputs are sufficient to generate the orientation selectivity in cortical cells (Nelso and others 1994). However, some other experiments showed that GABAergic antagonists

applied to cortical cells resulted in their equal responses to a bar at any orientation, indicating that intracortical inhibition plays an essential role in generating the orientation selectivity of cortical cells (Tsumoto and others 1979; Sillito and others 1980; Vidyasagar and others 1996).

These physiological results are supported by anatomical studies showing that the tectal cells projecting to an Imc cell are located in a dorsoventral column perpendicular to the horizontal axis adopted by Hamdi and Whitteridge (1954) (Figs 8 and 9). Because visual cells in the dorsal tectum have their ERF in the dorsal visual field, whereas those in the ventral tectum have ERF in the ventral visual field (Bilge 1971; Clarke and Whitteridge 1976; Gu and others 2000), dorsoventral distribution of the tectal cells projecting to an Imc cell predicts that the isthmic ERF should be elongated. According to the retinal representation of the visual field on the optic tectum (Hamdi and Whitteridge 1954; McGill and others 1966), the isthmic ERF must be oriented perpendicular to the horizontal meridian of the visual field. The present study combined electrophysiological and anatomical experiments to clearly show that the elongated ERF of an Imc cell is constructed from aligned circular tectal ERF and responsible for most of orientation selectivity and that intranuclear inhibitory circuits are responsible for sharpening the orientation tuning of the Imc cell. It appears that the Hubel–Wiesel feedforward model of RFs is also held for the visual system in nonmammals such as birds.

Notes

This work was supported by the National Natural Science Foundation of China and by the Chinese Academy of Sciences. *Conflict of Interest:* None declared.

Address correspondence to Shu-Rong Wang, Laboratory for Visual Information Processing, Institute of Biophysics, Chinese Academy of Sciences, 15 Datun Road, Beijing 100101, People's Republic of China. Email: wangsr@sun5.ibp.ac.cn.

References

- Bilge M. 1971. Electrophysiological investigations on the pigeon's optic tectum. *Q J Exp Physiol* 56:242–249.
- Britto LR, Gasparotto OC, Hamassaki DE. 1990. Visual telencephalon modulates directional selectivity of accessory optic neurons in pigeons. *Vis Neurosci* 4:3–10.
- Cao P, Gu Y, Wang SR. 2004. Visual neurons in the pigeon brain encode the acceleration of stimulus motion. *J Neurosci* 24:7690–7698.
- Chapman B, Zahs KR, Stryker MP. 1991. Relation of cortical cell orientation selectivity to alignment of receptive fields of the geniculocortical afferents that arborize within a single orientation column in ferret visual cortex. *J Neurosci* 11:1347–1358.
- Clarke PGH, Whitteridge D. 1976. The projection of the retina, including the “red area”, onto the optic tectum of the pigeon. *Q J Exp Physiol* 61:351–358.
- Erichsen JT, Hodos W, Evinger C, Bessette BB, Phillips SJ. 1989. Head orientation in pigeon: postural, locomotor and visual determinants. *Brain Behav Evol* 33:268–278.
- Ferster D, Chung S, Wheat H. 1996. Orientation selectivity of thalamic input to simple cells of cat visual cortex. *Nature* 380:249–252.
- Ferster D, Miller KD. 2000. Neural mechanisms of orientation selectivity in the visual cortex. *Annu Rev Neurosci* 23:441–471.
- Frost BJ, Scillely PL, Wong SCP. 1981. Moving background patterns reveal double-opponency of directionally specific pigeon tectal neurons. *Exp Brain Res* 43:173–185.
- Fu YX, Gao HF, Guo MW, Wang SR. 1998. Receptive field properties of visual neurons in the avian nucleus lentiformis mesencephali. *Exp Brain Res* 118:279–285.
- Gu Y, Wang Y, Wang SR. 2000. Regional variation in receptive field properties of tectal neurons in pigeons. *Brain Behav Evol* 55:221–228.
- Gu Y, Wang Y, Wang SR. 2001. Directional modulation of visual responses of pretectal neurons by accessory optic neurons in pigeons. *Neuroscience* 104:153–159.
- Güntürkün O, Remy M. 1990. The topographical projection of the nucleus isthmi pars parvocellularis (Ipc) onto the tectum opticum in the pigeon. *Neurosci Lett* 111:18–22.
- Hamdi FA, Whitteridge D. 1954. The representation of the retina on the optic tectum of the pigeon. *Q J Exp Physiol* 39:111–119.
- Hellon RF. 1971. The marking of electrode tip positions in nervous tissue. *J Physiol (Lond)* 214:12.
- Hubel DH, Wiesel TN. 1962. Receptive fields, binocular interaction and functional architecture in the cat visual cortex. *J Physiol (Lond)* 160:106–154.
- Hunt SP, Künzle H. 1976. Observations on the projections and intrinsic organization of the pigeon optic tectum: an autoradiographic study based on anterograde and retrograde, axonal and dendritic flow. *J Comp Neurol* 170:153–172.
- Jassik-Gerschenfeld D, Guichard J. 1972. Visual receptive fields of single cells in the pigeon's optic tectum. *Brain Res* 40:303–317.
- Karten HJ. 1969. The organization of the avian telencephalon: some speculations on the phylogeny of the amniote telencephalon. *Ann N Y Acad Sci* 167:164–180.
- Karten HJ, Hodos W. 1967. A stereotaxic atlas of the brain of the pigeon (*Columba livia*). Baltimore, MD: Johns Hopkins Press.
- McGill JI, Powell TPS, Cowan WM. 1966. The retinal representation upon the optic tectum and isthmo-optic nucleus in the pigeon. *J Anat* 100:5–33.
- Nelson S, Toth L, Sheth B, Sur M. 1994. Orientation selectivity of cortical neurons during intracellular blockade of inhibition. *Science* 265:774–777.
- Qu T, Dong K, Sugioka K, Yamadori T. 1996. Demonstration of direct input from the retina to the lateral habenular nucleus in the albino rat. *Brain Res* 709:251–258.
- Reid RC, Alonso JM. 1995. Specificity of monosynaptic connections from thalamus to visual cortex. *Nature* 378:281–284.
- Reiner A, Perkel DJ, Bruce LL, Butler AB, Csillag A, Kuenzel W, Medina L, Paxinos G, Shimizu T, Striedter G, Wild M, Ball GF, Durand S, Gunturkun O, Lee DW, Mello CV, Powers A, White SA, Hough G, Kubikova L, Smulders TV, Wada K, Dugas-Ford J, Husband S, Yamamoto K, Yu J, Siang C, Jarvis ED. 2004. Revised nomenclature for avian telencephalon and some related brainstem nuclei. *J Comp Neurol* 473:377–414.
- Shimizu T, Bowers AN. 1999. Visual circuits of the avian telencephalon: evolutionary implications. *Behav Brain Res* 98:183–191.
- Sillito AM, Kemp JA, Milson JA, Berardi N. 1980. A re-evaluation of the mechanisms underlying simple cell orientation selectivity. *Brain Res* 194:517–520.
- Tömböl T, Alpar A, Eyre MD, Németh A. 2006. Topographical organization of projections from the nucleus isthmi magnocellularis to the optic tectum of the chick brain. *Anat Embryol* 211:119–128.
- Tömböl T, Németh A. 1998. GABA-immunohistological observations, at the electron-microscopical level, of the neurons of isthmic nuclei in chicken, *Gallus domesticus*. *Cell Tissue Res* 291:255–266.
- Tsumoto T, Eckart W, Creutzfeldt OD. 1979. Modification of orientation sensitivity of cat visual cortex neurons by removal of GABA-mediated inhibition. *Exp Brain Res* 34:351–363.
- Varoqueaux F, Poulain P. 1994. Lateral septal projections onto tubero-infundibular neurons in the hypothalamus of the guinea pig. *Cell Tissue Res* 278:217–225.
- Vercelli A, Repici M, Garbossa D, Grimaldi A. 2000. Recent techniques for tracing pathways in the central nervous system of developing and adult mammals. *Brain Res Bull* 51:11–28.
- Vidyasagar TR, Pei X, Volgushev M. 1996. Multiple mechanisms underlying the orientation selectivity of visual cortical neurons. *Trends Neurosci* 19:272–277.
- Wang SR. 2003. The nucleus isthmi and dual modulation of the receptive field of tectal neurons in non-mammals. *Brain Res Rev* 41:13–25.

- Wang SR, Wang YC, Frost BJ. 1995. Magnocellular and parvocellular divisions of pigeon nucleus isthmi differentially modulate visual responses in the tectum. *Exp Brain Res* 104:376-384.
- Wang Y, Luksch H, Brecha NC, Karten HJ. 2006. Columnar projections from the cholinergic nucleus isthmi to the optic tectum in chicks (*Gallus gallus*): a possible substrate for synchronizing tectal channels. *J Comp Neurol* 494:7-35.
- Wang Y, Major DE, Karten HJ. 2004. Morphology and connections of nucleus isthmi pars magnocellularis in chicks (*Gallus gallus*). *J Comp Neurol* 469:275-297.
- Wang Y, Xiao J, Wang SR. 2000. Excitatory and inhibitory receptive fields of tectal cells are differentially modified by magnocellular and parvocellular divisions of the pigeon nucleus isthmi. *J Comp Physiol A* 186:505-511.
- Wang YC, Frost BJ. 1991. Visual response characteristics of neurons in the nucleus isthmi parvocellularis of pigeons. *Exp Brain Res* 87:624-633.
- Wu LQ, Niu YQ, Yang J, Wang SR. 2005. Tectal neurons signal impending collision of looming objects in the pigeon. *Eur J Neurosci* 22:2325-2331.
- Yang J, Li X, Wang SR. 2002. Receptive field organization and response properties of visual neurons in the pigeon nucleus semilunaris. *Neurosci Lett* 331:179-182.